12,09

Physicochemical properties and antioxidant activity of maltodextrin-coated cerium oxide nanoparticles

© S.A. Maslova[1,2], I.N. Bazhukova[1], A.V. Myshkina[1], E.O. Baksheev[1], M.O. Pronina[1], M.A. Mashkovtsev[1], A.S. Farlenkov[3]

[1] Ural Federal University after the first President of Russia B.N. Yeltsin, Yekaterinburg, Russia
[2] M.N. Mikheev Institute of Metal Physics, Ural Branch, Russian Academy of Sciences, Yekaterinburg, Russia
[3] Institute of High-Temperature Electrochemistry, Ural Branch, Russian Academy of Sciences, Yekaterinburg, Russia

E-mail: i.n.sedunova@urfu.ru

Received July 8, 2021
Revised July 13, 2021
Accepted July 16, 2021

The study on physicochemical properties of maltodextrin-coated cerium oxide nanoparticles was carried out. The surface structure and properties of CeO_2 nanoparticles were investigated. The ability of CeO_2 nanoparticles to perform the functions of catalase and peroxidase enzymes, as well as to inactivate hydroxyl radicals was shown.

Keywords: nanoparticles, cerium oxide, catalytic activity, antioxidant activity.

DOI: 10.21883/PSS.2022.14.54325.20s

1. Introduction

Nanoparticles of cerium oxide CeO_2 are a promising object for applications in medicine and biology. The biomedical application of nanoparticles is based on their inherent high oxygen nonstoichiometry, which determines their biological activity, as well as the absence of toxicity in living systems [1–3]. The presence of mixed valence states and oxygen vacancies on the surface of these nanoparticles affects their ability to participate in redox processes in the cell and exhibit catalytic, antioxidant, and other types of biological activity.

The high biological activity of nanocrystalline cerium oxide is associated primarily with the structure of its crystal lattice. Cerium is rare-earth metal from the lanthanide group, exhibiting oxidation states +3 and +4, the corresponding cerium oxides — Ce_2O_3 and CeO_2. The crystal lattice of cerium oxide CeO_2 is a cubic face-centered lattice, each oxygen atom is located in the center of a tetrahedron, the vertices of which are four cerium atoms. With a decrease in particle size, in contrast to many substances, for cerium oxide, an increase in the lattice cell parameter of the crystal lattice is observed. At the transition to the nanocrystalline state, the surface oxygen atom leaves the lattice and leaves two electrons, which are localized in the inner shell of the two nearest cerium atoms, making the transition from Ce^{4+} to Ce^{3+} [4]. The ionic radius of Ce^{3+} (0.1143 Å) is greater than the ionic radius of Ce^{4+} (0.097 Å), which explains the expansion of the crystal lattice.

Thus, the formation of oxygen vacancies in the structure of nanocrystalline cerium oxide CeO_2 leads to an increase in the fraction of Ce^{3+} atoms on the particle surface and an increase in oxygen nonstoichiometry. Nanocrystalline cerium oxide is a structure „core in a shell“, where the core is cerium oxide CeO_2, which is close to stoichiometric, and the surface is close in composition to Ce_2O_3. In other words, the oxygen nonstoichiometry increases from the center to the periphery [5]. This structure determines the activity of cerium oxide nanoparticles in redox processes. Due to the high oxygen nonstoichiometry, nanoparticles are able to bind reactive oxygen-containing compounds and radicals that are detrimental to living systems. In a number of works it has been demonstrated that CeO_2 nanoparticles exhibit multi-enzymatic activity, performing the functions of various enzymes: superoxide dismutase, catalase, peroxidase, oxidase [1,5–7].

The efficiency of using CeO_2 nanoparticles in medicine largely depends on the method and conditions of their synthesis, since they determine the size, morphology, and physicochemical properties of nanoparticles, and, consequently, their biological activity. In addition, the precursors and stabilizers used in the synthesis can affect the biocompatibility of nanoparticles and their toxicity in living systems. Therefore, when selecting a method for the synthesis of nanoparticles for medical use, it is required to simultaneously take into account a lot of factors that affect the properties of nanoparticles, their activity, and behavior in biological systems. Since the use of nanoparticles in biomedical practice requires their stable aggregate-resistant sols [8], various additives or coatings are used in their synthesis to increase the solubility and stability of colloidal solutions of nanoparticles. As stabilizers in the synthesis, most often substances are used that can be adsorbed on the surface of nanoparticles, or organic compounds that

play the role of a framework, between the elements of which nanoparticles are located. One of the most promising materials for stabilizing nanoparticles are low molecular glucans containing 2−20 structural elements in the chain [9]. Interest in the use of these materials is due to the biopolymer molecules being able to simultaneously control the size of the resulting nanoparticles during synthesis and act as colloidal stabilizers of highly dispersed sols of nanoparticles. At the same time, it is noted that the redox properties of CeO_2 nanoparticles stabilized by polysaccharide molecules are completely preserved [10]. By now, technologies for the synthesis of CeO_2 nanoparticles in the following biopolymer shells are known: dextran, pullulan, starch, chitosan, etc. [11].

However, there are only fragmentary literature data on the study of the physical and chemical properties and antioxidant activity of CeO_2 nanoparticles in a biopolymer shell of maltodextrin polysaccharide. Maltodextrin is a product of incomplete acid or enzymatic hydrolysis of potato or corn starch and is used in the production of food supplements, as it is a safe component. Therefore, this biopolymer is of interest for use as a colloidal stabilizer for nanoparticle sols, which are planned to be used in biomedical practice. The aim of this work is to study the morphology, physical and chemical properties, and biological activity of maltodextrin-stabilized cerium oxide nanoparticles.

2. Experiment details

Nanoparticles of cerium oxide CeO_2 in a maltodextrin shell were obtained by precipitation according to the procedure presented in the works [12,13]. The starting reagents were: cerium (III) nitrate solution ($Ce(NO_3)_3 \cdot xH_2O$), ammonia solution NH_4OH, maltodextrin (MD) with dextrose equivalent 10−12, isopropyl alcohol absolute, distilled water. All reagents are of analytical grade (mass fraction of impurities is maximum 0.05%). To prepare the initial solution, maltodextrin was dissolved in distilled water at room temperature and a solution of cerium nitrate was introduced while observing the molar ratio of the components $Ce:MD = 1:4$. An aqueous solution of ammonia was used as a precipitant.

The surface morphology and particle size of the synthesized cerium oxide nanocrystalline powders were studied by scanning electron microscopy (SEM) using an electron microscope X-Act ADD + JSM-5900LV (Jeol, Japan) equipped with a wave-dispersive microanalyzer, a lock chamber and an INCA Energy 250 and INCA Wave 500 electromagnetic interference suppression device. Micrographs of the surface of the material under study were obtained using detectors of back-scattered electrons (BSE mode) and secondary electrons (SE mode). W cathode was used as a source of electrodes, the accelerating voltage was 10 kV.

Nanoparticle sols were used to study the luminescent-optical properties and antioxidant activity. Nanoparticles were dispersed in distilled water and sonicated. Optical absorption spectra were measured using a Helios Alpha spectrophotometer ($\lambda = 190-1000$ nm) equipped with Vision 32 software. The calculation of the nanocrystal band gap was carried out by the Tauc graphical method [14]. Time dependences of the optical density of nanoparticle sols at certain wavelengths were measured using a PE-5400UF spectral photometer („EKROSKHIM"). The photoluminescence (PL) spectra of CeO_2 nanoparticles were measured using a Cary Eclipse (Agilent) fluorescent spectral photometer. The PL spectra were not corrected for the spectral sensitivity of the optical path.

The antioxidant activity of cerium oxide nanoparticles was evaluated by their ability to mimic the behavior of catalase and peroxidase enzymes, as well as the ability to inactivate hydroxyl radicals. The catalase mimetic activity of CeO_2 nanoparticles was studied by measuring the optical density of nanoparticle sols before and after the addition of hydrogen peroxide H_2O_2 [15]. The peroxidase mimetic activity of the nanoparticles was determined using a buffer solution containing 3.3′, 5.5′-tetramethylbenzidine (TMB) and hydrogen peroxide H_2O_2 [16]. To determine the ability of the studied CeO_2 nanoparticles to inhibit hydroxyl radicals, we used the property of the methyl violet (MV) dye to discolor under the action of $OH^{\bullet}$-radicals [16].

3. Experimental results and discussion

3.1. Morphology of maltodextrin-stabilized cerium oxide nanoparticles

The structure and surface properties of nanoparticles are the main factors that determine their biological activity in living systems. These characteristics affect the surface charge of nanoparticles, their sizes, the aggregative stability of sols, which determine the functional properties of nanoparticles, as well as their potential toxicity.

Figure 1 shows electron micrographs of the CeO_2 nanocrystalline powder synthesized with (*a*) and without (*b*) maltodextrin at different magnifications. Microscopic analysis showed that the CeO_2 nanocrystalline powder consists of agglomerates with sizes on the order of several hundreds of micrometers. Most of the agglomerates are polysaccharides that are part of maltodextrin (dextrin, glucose, maltose), and cerium ions are located on the surface of the polysaccharide chain. The shape of the nanoparticles is close to spherical. It should be taken into account that maltodextrin, used as a stabilizer in the synthesis of nanoparticles, can significantly change their shape, size, and other characteristics. Therefore, to study its effect on the surface morphology of nanoparticles, micrographs of CeO_2 nanocrystalline powder synthesized by a similar procedure, but without the use of maltodextrin, were obtained. As can be seen from Fig. 1, *b*, CeO_2 nanoparticles without a polysaccharide shell have dimensions of the order

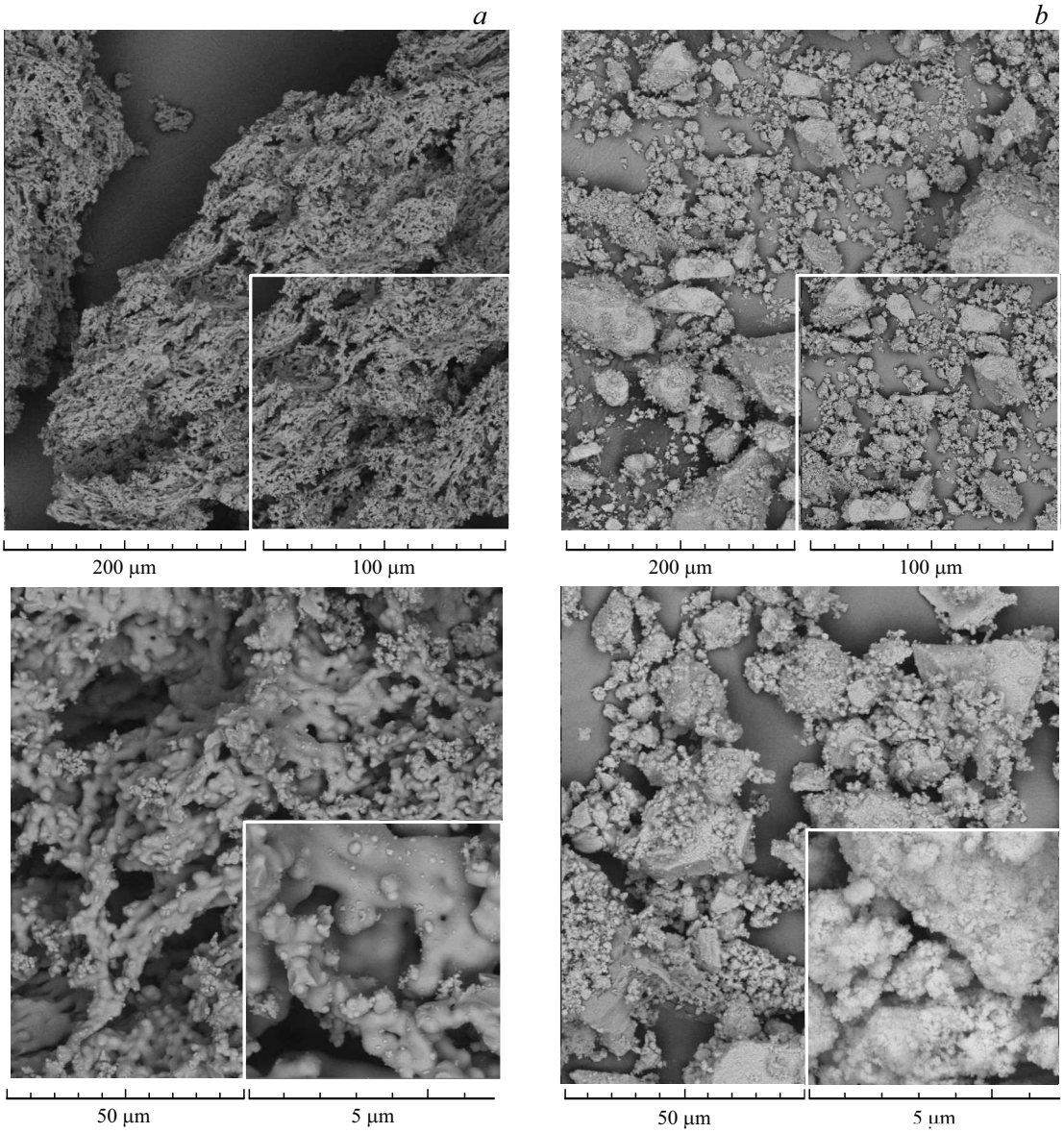

Figure 1. SEM electron micrographs of CeO_2 nanoparticles synthesized using (a) and without (b) maltodextrin.

of ten nanometers; however, due to the absence of a stabilizer, they stick together and form large agglomerates. Thus, the polysaccharide maltodextrin provides a fairly good aggregative stability of nanoparticles.

3.2. Luminescent-optical properties of sols of cerium oxide nanoparticles stabilized with maltodextrin

The application of biopolymer molecules in the synthesis of CeO_2 nanoparticles allows to simultaneously control the size of the resulting nanoparticles and stabilize highly dispersed aqueous sols [11,13]. Therefore, it can be assumed that, as a result of synthesis, CeO_2 nanoparticles stabilized by maltodextrin will be characterized by a pronounced oxygen nonstoichiometry and, accordingly, the presence of crystal lattice defects. The formation of the following defects is typical for cerium oxide nanoparticles: oxygen vacancies and related F^0, F^+ and F^{++}-centers, Ce^{3+} ions associated with the presence of oxygen vacancies, charge-transfer complexes $Ce^{4+}-O^{2-}$ [17]. Some defect centers have optical activity and can be detected by optical spectroscopy.

Figure 2, a shows the optical absorption spectra of sols of cerium oxide and maltodextrin nanoparticles. The optical absorption spectrum of the sol of CeO_2 nanoparticles is characterized by an intense absorption band in the range of 220–400 nm with a maximum at $\lambda \approx 270$ nm. This band may be due to photo-induced optical transitions with charge transfer from the $2p$-orbital of oxygen to the unfilled $4f$-orbital of the Ce^{4+} [18].

Since the nanoparticles under study are covered with a maltodextrin shell, which can also absorb radiation in this

wavelength range, it is important to evaluate the contribution of maltodextrin to the obtained spectrum. To do this, under similar conditions, the spectrum of a maltodextrin solution with a concentration equal to its concentration in the sol of nanoparticles was measured (Fig. 2, *a*, dashed line). It can be seen that maltodextrin practically does not absorb radiation in the studied wavelength range. This fact indicates the opportunity of using the method of optical spectroscopy to study the properties of nanoparticles and their changes that occur upon interaction with reactive oxygen species.

The obtained spectral data can also be used to determine the nanocrystal band gap E_g. To do this, according to the Tauc method, the optical absorption spectrum of CeO_2 nanoparticles was rearranged in the coordinates $(\alpha h\nu)^2$ from $h\nu$, where α — absorption coefficient, $h\nu$ — light quantum energy [19]. Figure 2, *b* shows the results of the graphical determination of the band gap E_g. According to the data obtained, the value of the band gap for direct-gap transitions was 3.4 eV.

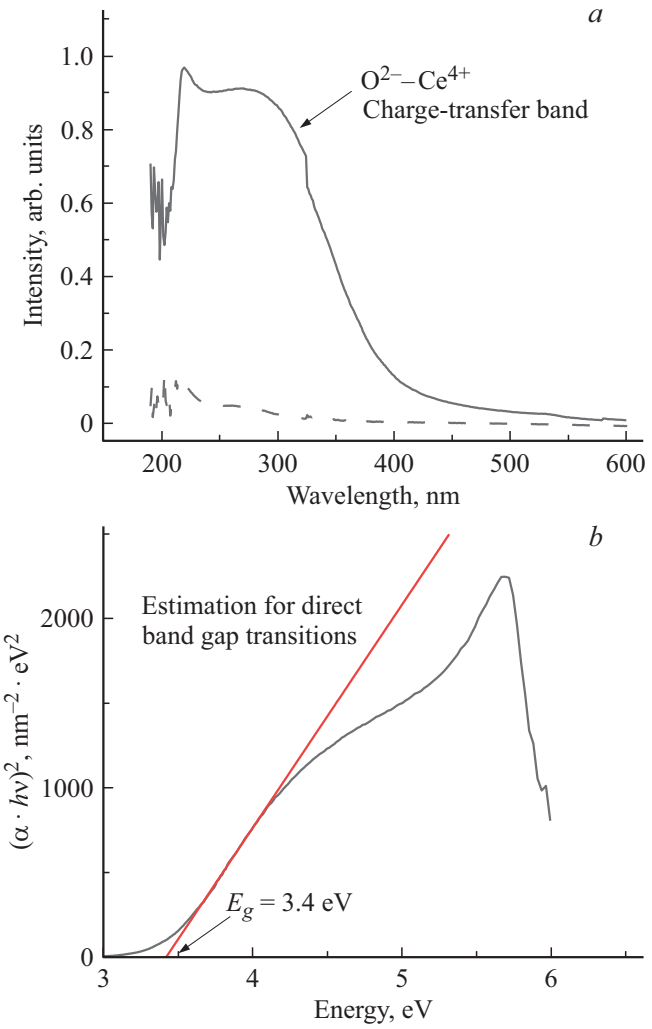

Figure 2. (*a*) Optical absorption spectra of sols of CeO_2 nanoparticles (solid line) and maltodextrin solution (dashed line). (*b*) An estimate of the band gap for direct-gap transitions in CeO_2 nanoparticles.

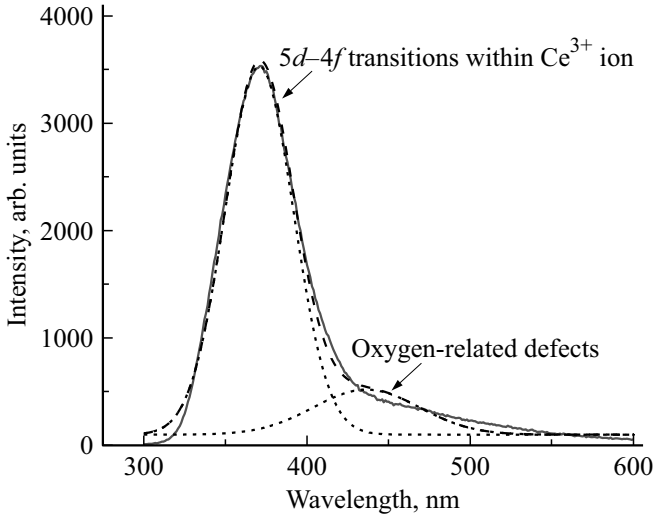

Figure 3. Photoluminescence spectrum of a sol of CeO_2 nanoparticles upon excitation $\lambda_{ex} = 250$ nm. The dotted lines show the selected Gaussian elementary bands, the dashed line shows the approximating curve.

Figure 3 shows the photoluminescence (PL) spectrum of a sol of cerium oxide nanoparticles measured upon excitation $\lambda_{ex} = 250$ nm. In the visible area, the luminescence spectrum is represented by a wide non-elementary PL band extending in the range from 350 to 600 nm, with a maximum in the area of 370 nm. The results of the decomposition of the PL spectrum indicate the presence of two overlapping main elementary Gaussian bands. The observed emission at 370 nm is probably related to the $5d \rightarrow 4f$ radiative transitions in Ce^{3+} ions. The presence of a wide low-intensity luminescence band in the area of 400–500 nm can be associated with the formation of optically active defects associated with oxygen vacancies on the surface of nanoparticles [18].

On the basis of the performed analysis, it can be concluded that the CeO_2 nanoparticles stabilized by maltodextrin are small in size and, correspondingly, their strong oxygen nonstoichiometry. This structure determines the activity of cerium oxide nanoparticles in redox processes. Thus, in particular, CeO_2 nanoparticles are able to bind reactive oxygen-containing compounds and radicals that are detrimental to living systems, i.e. exhibit antioxidant properties.

3.3. Catalase mimetic activity of nanoparticles

Hydrogen peroxide H_2O_2 is one of the reactive oxygen species and is neutralized by the enzyme catalase. To study the catalase mimetic activity of CeO_2 nanoparticles, we analyzed the changes occurring in their optical absorption spectra after interaction with hydrogen peroxide (Fig. 4, *a*).

According to the presented spectra, the addition of H_2O_2 nanoparticles to the sol leads to a shift of the absorption

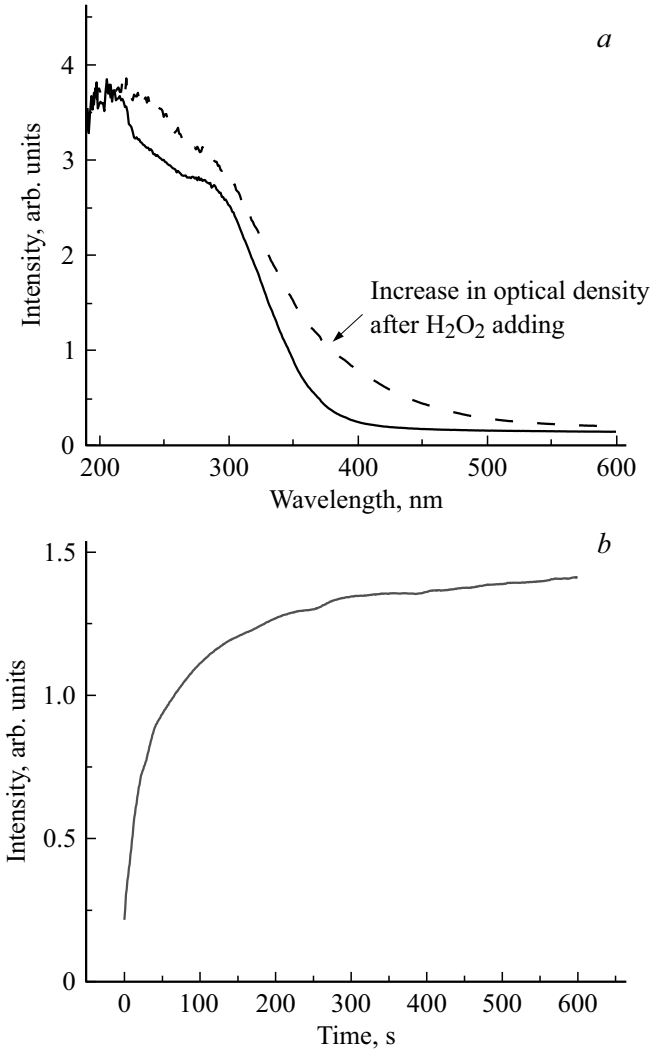

Figure 4. Study of the catalase mimetic activity of sols of CeO_2 nanoparticles: *a* — optical absorption spectra of sols of CeO_2 nanoparticles before and after the addition of hydrogen peroxide H_2O_2 (solid and dashed lines, respectively); *b* — time dependence of the optical density of the nanoparticle sol at a wavelength $\lambda = 400$ nm after the addition of hydrogen peroxide H_2O_2.

edge to the area of longer wavelengths (Fig. 4, *a*). It is known that the position of the bands in the optical absorption spectrum of CeO_2 nanoparticles containing mixed valence states Ce^{3+} and Ce^{4+} depends on the ratio Ce^{3+}/Ce^{4+} [20], while an increase in the relative content of Ce^{3+} ions leads to a blue shift of the absorption band [21]. In the obtained spectra, on the contrary, a shift of the absorption edge towards the red wavelength range is observed. An additional confirmation of the change in the Ce^{3+}/Ce^{4+} valence ratio towards an increase in the proportion of Ce^{4+} ions in the interaction processes is the change in the color of the nanoparticle sol from pale to bright yellow after the introduction of hydrogen peroxide. The appearance of a yellow color of the sol in this case may be due to the absorption of radiation by Ce^{4+} ions in this area. At the same time, during the experiment, the change in the color of the sol occurred almost instantly after adding H_2O_2 to it (Fig. 4, *b*), which indicates a fast rate of the processes of interaction of nanoparticles with this reactive oxygen species.

The increase in the absorption intensity of CeO_2 nanoparticles after the addition of H_2O_2 in the range of 300–450 nm can be associated both with an increase in the number of ions Ce^{4+}, and with the formation of adsorbed forms of oxygen on the surface of nanoparticles (for example, hydroperoxide), which absorb radiation in this area [22]. It is also impossible to exclude the simultaneous occurrence of these processes, in which the formation of oxidation products is accompanied by a change in the oxidation state of cerium.

3.4. Peroxidase mimetic activity of nanoparticles

In contrast to catalase, the substrate of the peroxidase enzyme is not only hydrogen peroxide itself, but also inorganic or organic molecules that are oxidized by hydrogen peroxide in the presence of this enzyme. Thus, peroxidase is a redox enzyme. Peroxidase regulates the level of hydrogen peroxide, using it as an electron acceptor while participating in the oxidation of biological substrates. Peroxidase cannot be fully called an antioxidant, however, according to [23], antioxidants and peroxidase are part of a single antioxidant defense system and control each other's levels.

To study the peroxidase mimetic activity of CeO_2 nanoparticles, in this study, we analyzed the changes that occur in the spectra of a solution of 3, 3′, 5, 5′-tetramethylbenzidine (TMB) after the addition of peroxide hydrogen H_2O_2 and a sol of CeO_2 nanoparticles (Fig. 5, *a*). During the reaction catalyzed by peroxidase, TMB is oxidized to a product that has a blue color and an absorption maximum at 652 nm (Fig. 5, *a*). Figure 5, *b* shows the time dependence of the optical density of a TMB solution and hydrogen peroxide H_2O_2 at a wavelength of $\lambda = 652$ nm after adding a CeO_2 nanoparticle sol with different concentrations (25 and 50 μg/ml). It can be seen that the TMB oxidation reaction in the presence of H_2O_2 and CeO_2 nanoparticles proceeds very rapidly in the first minutes, then tends to saturation.

It is assumed that the peroxidase activity of CeO_2 nanoparticles is associated with the formation of adsorbed oxygen species on their surface as a result of interaction with hydrogen peroxide. It is noted that the formation of such peroxo- or hydroperoxo forms causes the oxidation of TMB [16,24]. Thus, we can conclude that CeO_2 nanoparticles are capable of imitating the behavior of the peroxidase enzyme.

3.5. The ability of nanoparticles to inactivate hydroxyl radicals

Among all reactive oxygen species, the most reactive is the hydroxyl radical. The ability of CeO_2 nanoparticles to

inactivate the action of these radicals was studied using the methyl violet dye, which changes its color intensity upon reaction with $OH^{\bullet}$-radicals. To obtain $OH^{\bullet}$-radicals, the Fenton reaction was used, according to which their formation occurs in biological systems (during the interaction of ferrous iron salt $FeSO_4$ and hydrogen peroxide H_2O_2). Figure 6, *a* shows the optical absorption spectra of a methyl violet dye solution (solid line), as well as MV solutions after the addition of iron sulfate $FeSO_4$ and hydrogen peroxide H_2O_2 (dashed line) and $FeSO_4$, H_2O_2 and nanoparticle sol CeO_2 (dotted line). The addition of $FeSO_4$ and H_2O_2 to a solution of methyl violet leads to a decrease in the absorption intensity in the range of 480–620 nm, which is due to with the formation of hydroxyl radicals as a result of the Fenton reaction and the discoloration of the dye solution under their action (Fig. 6, *a*, dashed line). The introduction of a sol of nanoparticles into a solution leads to a decrease in the degree of dye degradation and a higher value of the optical density of the solution at 585 nm (Fig. 6, *a*, dotted line).

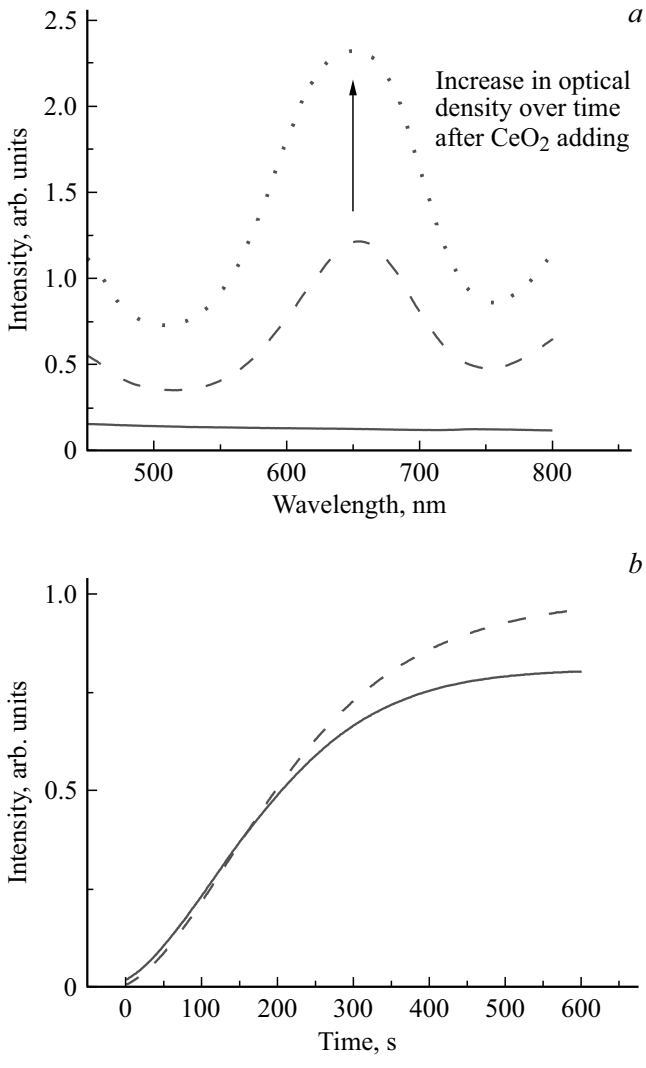

Figure 5. Study of peroxidase mimetic activity of sols of CeO_2 nanoparticles: *a* — optical absorption spectra of TMB solution and hydrogen peroxide H_2O_2 before (solid line) and after the addition of the sol of CeO_2 nanoparticles (dashed line — immediately after the addition of CeO_2, dotted line — through 5 min after adding CeO_2); *b* — time dependence of the optical density of the TMB solution and hydrogen peroxide H_2O_2 at the wavelength $\lambda = 652$ nm after addition of CeO_2 nanoparticle sols with different concentrations (25 μg/ml and 50 μg/ml — solid and dashed lines, respectively).

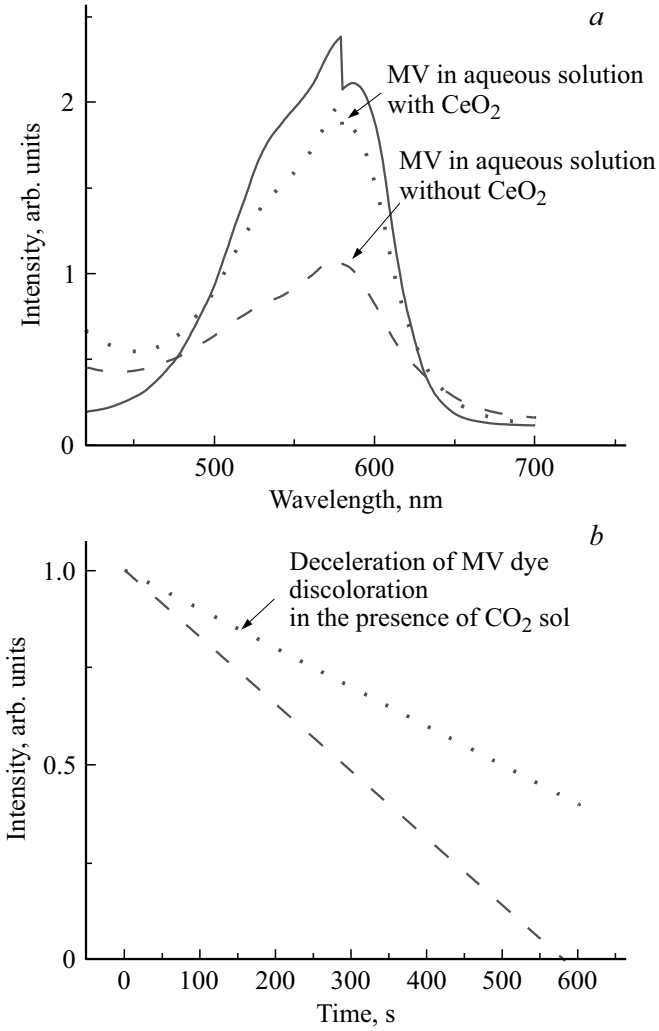

Figure 6. Study of the ability of CeO_2 nanoparticle sols to inactivate hydroxyl radicals: *a* — optical absorption spectra of MV dye solution (solid line), MV solution after addition of $FeSO_4$ and H_2O_2 (dashed line), MV solution after adding $FeSO_4$, H_2O_2 and a CeO_2 nanoparticle sol (dotted line); *b* — time dependence of the optical density of the MV solution at a wavelength $\lambda = 585$ nm after adding $FeSO_4$ and H_2O_2 (dashed line) and after addition of $FeSO_4$, H_2O_2 and nanoparticle sol CeO_2 (dotted line).

Figure 6, *b* shows the time dependence of the optical density of the MV solution at a wavelength $\lambda = 585$ nm after adding $FeSO_4$ and H_2O_2 (dashed line) and after addition of $FeSO_4$, H_2O_2 and nanoparticle sol CeO_2 (dotted line). It can be seen that the rate of discoloration of the MV solution with $FeSO_4$ and H_2O_2 slows down when the

sol of CeO_2 nanoparticles is added. Therefore, we can conclude that CeO_2 nanoparticles are able to absorb a part of $OH^{\bullet}$-radicals and thus protect the dye from their action.

The interaction of CeO_2 nanoparticles with the highly reactive $OH^{\bullet}$-radical occurs due to switching between two valence states Ce^{3+} and Ce^{4+}. Due to the ability of CeO_2 nanoparticles to self-regenerate, this process occurs continuously during the entire incubation period. In this case, the activity of nanoparticles is due to the presence of Ce^{3+} ions on their surface, which act as active centers of the enzyme [25].

4. Conclusion

In this work, we studied nanoparticles of cerium oxide CeO_2 obtained by precipitation and stabilized by a polysaccharide maltodextrin shell during synthesis. The study of cerium oxide nanoparticles was carried out using the methods of microscopic analysis, as well as optical and luminescent spectroscopy.

Microscopic analysis of the surface structure of CeO_2 cerium oxide nanocrystalline powders stabilized by maltodextrin showed that they consist of agglomerates with sizes of the order of several hundred μm, cerium ions are located on the surface of the polysaccharide chain. Based on the obtained micrographs, it can be argued that the synthesized nanoparticles have nanometer dimensions.

For the material under study, the formation of optically active centers responsible for optical absorption in the UV area and the observed luminescence was found. These defects are probably related to oxygen vacancies and the Ce^{3+} ions associated with them. Oxygen nonstoichiometry associated with the formation of Ce^{3+} ions on the particle surface probably determines the biological activity of the nanomaterial.

Based on the studies performed, it can be concluded that CeO_2 nanoparticles are capable of performing the functions of catalase and peroxidase enzymes and destroying hydrogen peroxide. In addition, it was demonstrated that CeO_2 nanoparticles are able to inactivate hydroxyl radicals similarly to molecular antioxidants (ascorbic acid, tocopherol, methionine, etc.). Thus, the studies performed have shown the fundamental possibility of using cerium oxide nanoparticles in medicine, for example, as potential antioxidants to protect cells from reactive oxygen species.

The use of cerium oxide nanoparticles as exogenous antioxidants to protect cells from oxidative stress requires a deep understanding of the mechanism of their catalytic activity. As of this date, potential reaction models have been proposed, but there is no single point of view on this issue, and the exact mechanism of the interaction of CeO_2 nanoparticles with reactive oxygen species remains unclear. Further studies of the relationship between the physicochemical properties and biological activity of cerium oxide nanoparticles are required. A more thorough study of this theme, the establishment of strict patterns and relationships will allow to implement a wide range of biomedical applications of nanocrystalline cerium oxide.

Acknowledgments

The authors thank V.V. Kasianova for her help and participation in the study.

Conflict of interest

The authors declare that they have no conflict of interest.

References

[1] A. Dhall, W. Self. Antioxidants **7**, *8*, 97 (2018).
[2] N. Thakur, P. Manna, J. Das. J. Nanobiotechnology **17**, *1*, 1 (2019).
[3] B. Nelson, M. Johnson, M. Walker, K. Riley, C. Sims. Antioxidants **5**, *2*, 15 (2016).
[4] N.V. Skorodumova, S.I. Simak, B.I. Lundqvist, I.A. Abrikosov, B. Johansson. Phys. Rev. Lett. **89**, *16*, 166601 (2002).
[5] A.B. Shcherbakov, O.S. Ivanova, N.Ya. Spivak, V.V. Kozik, V.I. Ivanov. Synthesis and biomedical applications of nanodispersed cerium dioxide. Publishing house of the Tomsk State University, Tomsk (2016). 476 p.
[6] Z. Lu, Y. Dang, C. Dai, Y. Zhang, P. Zou, H. Du, Y. Zhang, M. Sun, H. Rao, Y. Wang. J. Hazardous Mater. **403**, 123979 (2021).
[7] K.R.B. Singh, V. Nayak, T. Sarkar, R.P. Singh. RSC Advances. Royal Soc. Chem. **10**, *45*, 27194 (2020).
[8] M. Darroudi, M. Ahmad, A. Abdullah, N. Ibrahim. Int. J. Nanomedicine **6**, *1*, 569 (2011).
[9] A.B. Shcherbakov, N.M. Zholobak, V.K. Ivanov, O.S. Ivanova, A.V. Marchevsky, A.E. Baranchikov, N.Ya. Spivak, Yu.D. Tretyakov. Russ. J. Inorg. Chem. **57**, *11*, 1411 (2012).
[10] H. Yazici, E. Alpaslan, T.J. Webster. JOM **67**, *4*, 804 (2015).
[11] F. Charbgoo, M. Bin Ahmad, M. Darroudi. Int. J. Nanomedicine **12**, 1401 (2017).
[12] E.O. Baksheev, M.O. Pronina, M.A. Mashkovtsev, A.V. Myshkina, I.N. Bazhukova, V.V. Kasianova. AIP Conf. Proc. **2174**, 020156 (2019).
[13] A.B. Shcherbakov, N.M. Zholobak, V.K. Ivanov, O.S. Ivanova, A.V. Marchevsky, A.E. Baranchikov, N.Ya. Spivak, Yu.D. Tretyakov. Zhurn. neorgan. khimii **57**, *11*, 1499 (2012) (in Russian).
[14] J. Tauc. BMC Public Health **3**, *1*, 37 (1968).
[15] I. Bazhukova, I. Zvonareva, A. Myshkina, S. Bazhukov, I. Gavrilov, V. Meschaninov. NANOCON 2019 — Conference Proceedings. 11th Int. Conf. Nanomaterials. Res. Appl. 348 (2020).
[16] G. Vinothkumar, P. Arunkumar, A. Mahesh, A. Dhayalan, K. Suresh Babu. New J. Chem. Royal Soc. Chem. **42**, *23*, 18810 (2018).
[17] E.N. Okrushko, V.V. Seminko, P.O. Maksimuchuk, I.I. Bespalova, N.V. Kononets, O.G. Viagin, Yu.V. Malyukin. Low Temp. Phys. **43**, *5*, 636 (2017).
[18] A.I. Medalia, B.J. Byrne. Rev. Anal. Chem. **23**, *3*, 453 (1951).

[19] I.N. Bazhukova, A.V. Myshkina, S.Yu. Sokovnin, V.G. Ilves, A.N. Kiryakov, S.I. Bazhukov, R.A. Vazirov, V.V. Kasianova, I.A. Zvonareva. Physics of the Solid State **61**, *5*, 974 (2019).
[20] D. Damatov, J.M. Mayer. Chem. Commun. Royal Soc. Chem. **52**, *67*, 10281 (2016).
[21] S. Tsunekawa, T. Fukuda, A. Kasuya. J. Appl. Phys. **87**, *3*, 1318 (2000).
[22] A.L. Popov, A.B. Shcherbakov, N.M. Zholobak, A.Ye. Baranchikov, V.K. Ivanov. Nanosyst. Phys. Chem. Math. **8**, *6*, 760 (2017).
[23] V.V. Verkhoturov. Researched in Russia **4**, 605 (2001).
[24] V. Baldim, F. Bedioui, N. Mignet, I. Margaill, J.F. Berret. Nanoscale **10**, *15*, 6971 (2018).
[25] Y. Xue, Q. Luan, D. Yang, X. Yao, K. Zhou. J. Phys. Chem. **115**, *11*, 4433 (2011).